A MODEL BASED COMPUTER ANALYSIS OF CREEP DATA (CRISPEN): APPLICATIONS TO NICKEL-BASE SUPERALLOYS

A Barbosa^{1,2}, N G Taylor³, M F Ashby³, B F Dyson¹ and M McLean¹

- 1 Division of Materials Applications, National Physical Laboratory, Teddington, Middlesex TW11 OLW, UK
- 2 Imperial College of Science and Technology, Prince Consort Road, London, SW7 2BP, UK
- 3 University Engineering Department, University of Cambridge, Trumpington Street, Cambridge CB2 1PZ, UK

Abstract

The physical mechanisms of deformation and fracture that control the shapes of creep curves in superalloys are reviewed and creep by these mechanisms is modelled using the approach of continuum damage mechanics. The resulting constitutive and damage evolution laws for creep are thus fully compatible with the underlying physics of the process. The equation—sets are implemented in a computer system (CRISPEN) that operates on an IBM AT or SYSTEM 2 personal computer to allow: (a) analysis of creep curves; (b) compilation of a database representing full creep curve shapes; (c) simulation of creep curves for abitrary test conditions and (d) comparison of simulated curves with available data. CRISPEN has been applied successfully to a range of nickel—base superalloys (wrought, conventionally cast, directionally solidified, single crystal). Examples are given of the agreement between creep simulations and experimental data for both representations of isolated creep curves and extrapolations to different stress and/or temperature and to variable stress/temperature conditions.

Superalloys 1988 Edited by S. Reichman, D.N. Duhl, G. Maurer, S. Antolovich and C. Lund The Metallurgical Society, 1988

Introduction

Although considerable effort and expense have been directed to characterising the highly non-linear creep behaviour of engineering alloys, such as nickel-base superalloys, most current compilations of creep data for engineering design represent only simple measures of creep performance. Indicators such as rupture life, time to 1% extension, minimum creep rate and ductility are adequate for traditional design-to-code methods. However, advanced computer-aided design procedures will require an increasingly sophisticated description of the full strain-time evolution of the material during complex loading cycles. There have been many empirical analyses of the shapes of creep curves that have met with varying degrees of success, but these have had no clear physical basis and, consequently, cannot be extrapolated with confidence beyond the field of the database to predict either longer lives or the effects of typical service cycles.

The understanding of high temperature deformation and fracture of superalloys has developed to the point where the important mechanisms are believed to have been identified. Detailed models of the time dependent movement of dislocations around γ '-particles by cutting, bowing and climb have been proposed that have the potential of accounting for the principal features of the creep behaviour of these materials (1). Similarly, theories of the development of damage that leads to tertiary creep and fracture in these materials have been advanced (2,3). The purpose of the present study has been to translate this knowledge of the underlying physics of deformation and fracture into a constitutive description of the creep behaviour that can be readily used in engineering calculations. The principal aim of the programme has been to assess the viability of developing a computer-system, incorporating these physically-based constitutive laws, and a base of reliable data to provide a capability for describing the full shapes of creep curves and to predict creep behaviour under conditions for which data are not available. The approach adopted has been to use the formalism of continuum damage mechanics expressed in terms of state variables that have clear physical significance.

Mechanisms and Models

Creep curves for nickel-base superalloys do not exhibit a long steady state behaviour. Rather, after a short primary transient of progressively decreasing creep rate until a minimum value ϵ_{\min} is achieved, most of the life is characterised by an extensive period of tertiary-creep where the creep rate progressively increases. Consequently, we shall restrict the following discussion to the causes of primary and tertiary creep.

Primary creep

In simple single-phase alloys, the strength of the material is a consequence of the dislocation network within the material. Primary creep is the result of hardening due to an increase in dislocation density with increasing strain until a steady state is reached when recovery exactly balances the rate of hardening. The situation is rather different in multi-phase engineering alloys where primary creep can be caused by stress redistributions between the various heterogeneities in the material (eg between differently oriented grains, between soft matrix and hard particles). Ion et al⁽⁴⁾ have proposed a general model that describes the latter situation and is compatible with the successful empirical formulation of Webster et al⁽⁵⁾ which has similarities to the primary component of the θ -projection description of creep curves⁽⁶⁾.

$$\epsilon = \frac{\sigma}{-+\epsilon_{p}} \left\{ 1 - \exp(-D \dot{\epsilon}_{min} t) \right\} + \dot{\epsilon}_{min} t$$
 (1)

where E is Youngs modulus, ϵ_p is the total primary strain and D is a constant characterising the rate of hardening.

Tertiary creep

Ashby and Dyson⁽⁷⁾ have reviewed the range of phenomena that can lead to an acceleration in creep rate in the tertiary stage. The acceleration is caused by changes in external geometry and internal structure, with clear physical meaning, that can be defined as damage. For superalloys there appear to be three important types of damage that can contribute to tertiary creep and these are shown schematically in Figure 1.

Intrinsic softening of superalloys is associated with changes in the dislocation substructure. Dyson and McLean⁽²⁾ have analysed a wide range of creep data for superalloys and shown that creep softening results from accumulated plastic strain, rather than from a time dependent coarsening of the microstructure as had been previously advocated.⁽⁸⁾ They proposed that the accelerating creep rate was due to increasing dislocation densities and support for this view has been obtained from electron microscope studies.^(9,10) Ion et al⁽⁴⁾ have developed these ideas into strain softening models of tertiary creep. A linear strain softening model gives precisely the equation that accounts for the tertiary creep component of the θ -projection approach⁽⁶⁾.

$$\epsilon = \frac{1}{C_{\varrho}} \left[\exp \left(C_{\varrho} \ \dot{\epsilon}_{i} \ t \right) - 1 \right]$$
 (2)

where $\dot{\epsilon}_i$ is the initial creep rate and C_{ℓ} is a constant. An alternative exponential softening model⁽⁴⁾, which is used in the subsequent analysis, leads to the following equation.

$$\epsilon = -\frac{1}{C} \ln \left[1 - C \epsilon_i t \right]$$
 (3)

where C is also a constant.

b) Development of grain boundary cavitation causes a loss of internal load bearing section that leads to an increased stress on the remaining sound ligaments. Dyson and Gibbons(3) have examined the shapes of creep curves of nickel-based superalloys with different ductilities resulting from, for example, increased cavitation associated with detrimental trace element concentrations. They show that Equation 3 adequately describes the tertiary parts of the creep curves, but that C increases with decreasing fracture strain ϵ_f . They modelled this aspect of the behaviour showing that cavitation leads to an addition to the intrinsic strain softening constant of $\sim n/3 \epsilon_f$ where n is the stress exponent associated with the minimum creep rate.

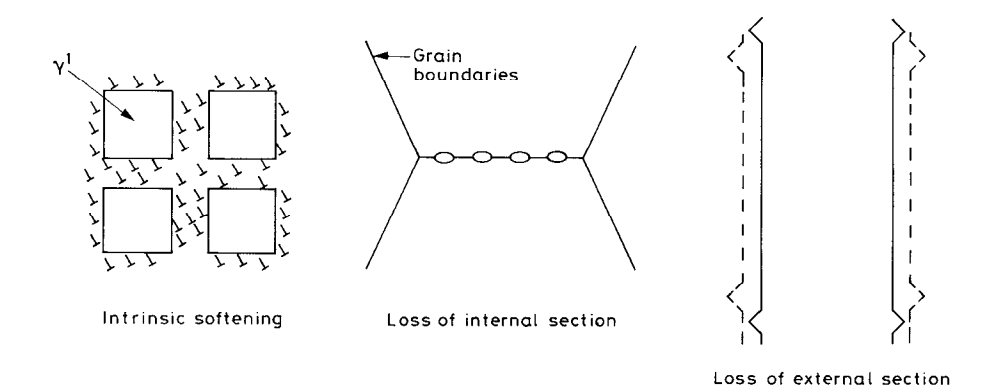


Figure 1 Schematic illustration of the three categories of micro—and macro-structural changes that cause tertiary creep in superalloys.

c) Loss of external section through the reduction in area of cross-section associated with tensile strain during constant load tests also leads to a progressive increase in stress and this causes strain rate acceleration. Assuming constant volume, the reduction in area dA scales with the change in strain $d \in Which$, for constant load, simply relates to the change in stress. Thus:

$$d\epsilon = -\frac{dA}{A} = \frac{d\sigma}{\sigma} \tag{4}$$

Integrating Equation 4 and combining it with a power-law representation of the initial creep rate, $\dot{\epsilon}_i = A \sigma^n$, leads to the following expression

$$\epsilon = -\frac{1}{n} \ln \left[1 - n\epsilon_i t \right]$$
 (5)

Equations 3 and 5 are clearly of the same form but with different constants.

Constitutive Laws and CRISPEN

In the approach of continuum damage mechanics, pioneered by Kachanov⁽¹¹⁾, and extended by several authors⁽¹²⁻¹⁴⁾, the creep rate at any instant is expressed as a function of both the operating conditions (σ,T) and of one or more state variables or damage parameters. Equations describing the evolution of the state variables (ω_1,ω_2) are also expressed in differential form and the creep behaviour is determined by integrating the coupled set of differential equations.

$$\dot{\epsilon} = f (\sigma, T, \omega_1, \omega_2, \dots)
\dot{\omega}_1 = g (\sigma, T, \omega_1, \omega_2, \dots)
\dot{\omega}_2 = h (\sigma, T, \omega_1, \omega_2, \dots)$$
(6)

In previous published $work^{(11-14)}$, the explicit forms of Equation 6 used to represent creep behaviour have been derived empirically. The important feature of the present study has been to derive explicit forms of Equation 6 that are consistent with the current understanding of deformation and fracture outlined in the previous section. By retaining the differential formulation and integrating numerically, it is relatively simple to consider the effect of variable loading conditions.

The primary creep behaviour can be considered to be due to the development of an internal stress σ_i , due to stress redistribution in the heterogeneous material. Taking as the state variable $S = \sigma_i/\sigma$ where σ is the applied stress we can write for the linearised form of the model⁽⁴⁾:

$$\dot{\epsilon} = \dot{\epsilon}_{min} \frac{(1-S)}{(1-S_{SS})}$$

$$\dot{S} = H\dot{\epsilon} - RS$$
(7)

where H,R are constants describing hardening and recovery respectively, S_{SS} is the steady state value of S and R = $H\dot{\epsilon}_{min}/S_{SS}$. Equations 7 integrate to exactly the form of Equation 1.

The tertiary creep behaviour can be represented by the following set of equations

$$\begin{array}{ccc}
\dot{\epsilon} & = & \dot{\epsilon}_{i} & e^{\omega} \\
\dot{\omega} & = & C\dot{\epsilon}
\end{array}$$
(8)

where $\dot{\epsilon}_i$ is the initial creep rate and the constant C is the sum of three terms representing intrinsic softening, loss of internal section and loss of external section (3). Thus:

$$C = C_{int} + \frac{1}{3} \frac{n}{\epsilon_f} + n$$
 (9)

Integration of Equations 8 leads to Equation 3.

When both primary and tertiary creep occur, a two state variable description is required. The two expressions describing $\dot{\epsilon}$ are combined in product (rather than addition) form to account for interactions between the two mechanisms; addition would imply that primary and tertiary creep were independent and co-existed throughout the entire creep life. Thus:

$$\dot{\epsilon} = \dot{\epsilon}_{i} (1-S) e^{\omega}$$

$$\dot{S} = H\dot{\epsilon} - \frac{H\dot{\epsilon}_{i}}{S_{SS}} S$$

$$\dot{\omega} = C\dot{\epsilon}$$
(10)

The four-parameter set ($\dot{\epsilon}_i$, S_{SS}, H, C) completely describes changes in the variables at a given loading condition and each may vary with stress and temperature.

A software package, designated CRISPEN, has been developed that utilises sets of equations such as Equation 10 to represent the full creep curves of engineering alloys. By analysing raw creep curves, a database of model parameters ($\dot{\epsilon}_i$, S_{SS} , H, C) can be constructed. Using this database, the strain/time evolution during arbitrary stress and temperature conditions can be simulated and, when available, compared with experimental data. The system is designed to allow interpolation and limited extrapolation to unknown conditions and to cope with variable stresses and temperatures. It has been written to operate on an IBM AT or SYSTEM 2 personal computer in order to facilitate dissemination. Consequently the analysis involves acceptable approximation consistent with limited memory available.

Data Analysis

Equation Sets 7 or 8 taken alone can be integrated analytically to describe primary and tertiary creep, but it has not proved possible to derive an analytical solution to the complete three-equation set (Equation 10). Consequently, derivation of the model parameters ($\dot{\epsilon}_i$, S_{SS} , H, C) from an arbitrary creep curve is not straight forward. Two different methods have been used with varying success depending on the nature of the creep curve.

- a) Method 1 depends on the analysis of the creep curve where strain ϵ is displayed as a function of time. As discussed by Ion et al⁽⁴⁾ the general shape of the creep curve can be represented by the four operational parameters (ϵ_p , t_p , $\dot{\epsilon}_{min}$, t_t) defined in Figure 2a. If primary creep is largely exhausted before significant strain rate acceleration occurs, then the model parameters required for subsequent calculation are simply related to these operational measures of the creep curve. This approach requires that $\dot{\epsilon}_{min} \sim \dot{\epsilon}_i$: where the inequality is not satisfied due to, for example, a dominant primary behaviour or distortion of these minimum creep rate by microstructural changes, then an alternative analysis is required.
- b) Method 2 analyses the differential form of the creep curve where strain rate $\dot{\epsilon}$ is displayed as a function of strain ϵ . The strain softening parameter $C = d\ln \dot{\epsilon}/d\epsilon$ when $S \to S_{SS}$. Although $\dot{\epsilon}_i \neq \dot{\epsilon}_{min}$, and indeed is not directly measurable from the creep curve, it can be estimated by the procedure indicated graphically in Figure 2b. The primary parameters can similarly be derived as described more fully by Taylor and Ashby⁽¹⁵⁾.

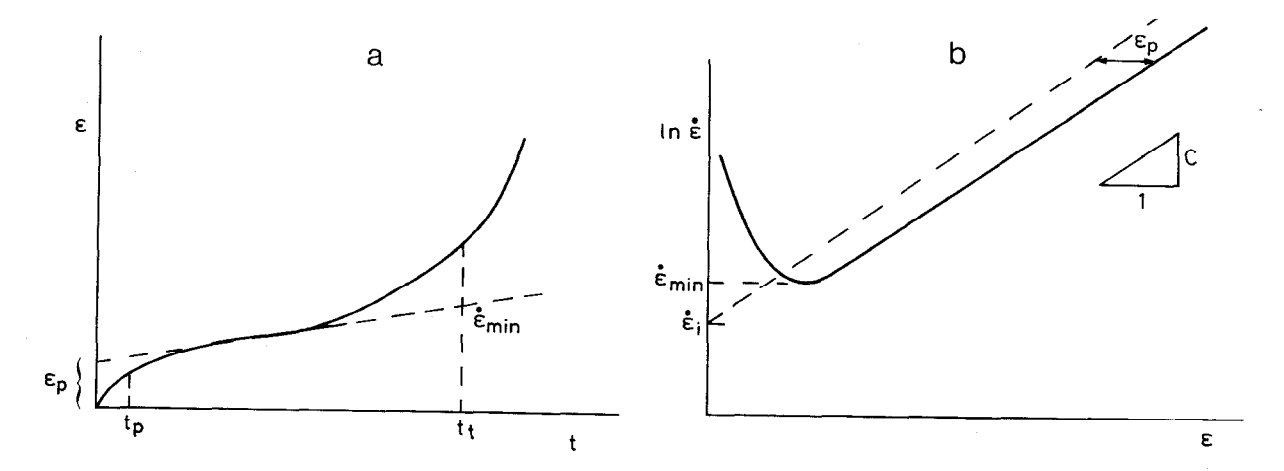


Figure 2 Schematic creep curves showing analysis procedures used in determining model parameters.

- a) strain versus time Method 1.
- b) log (strain rate) versus strain Method 2.

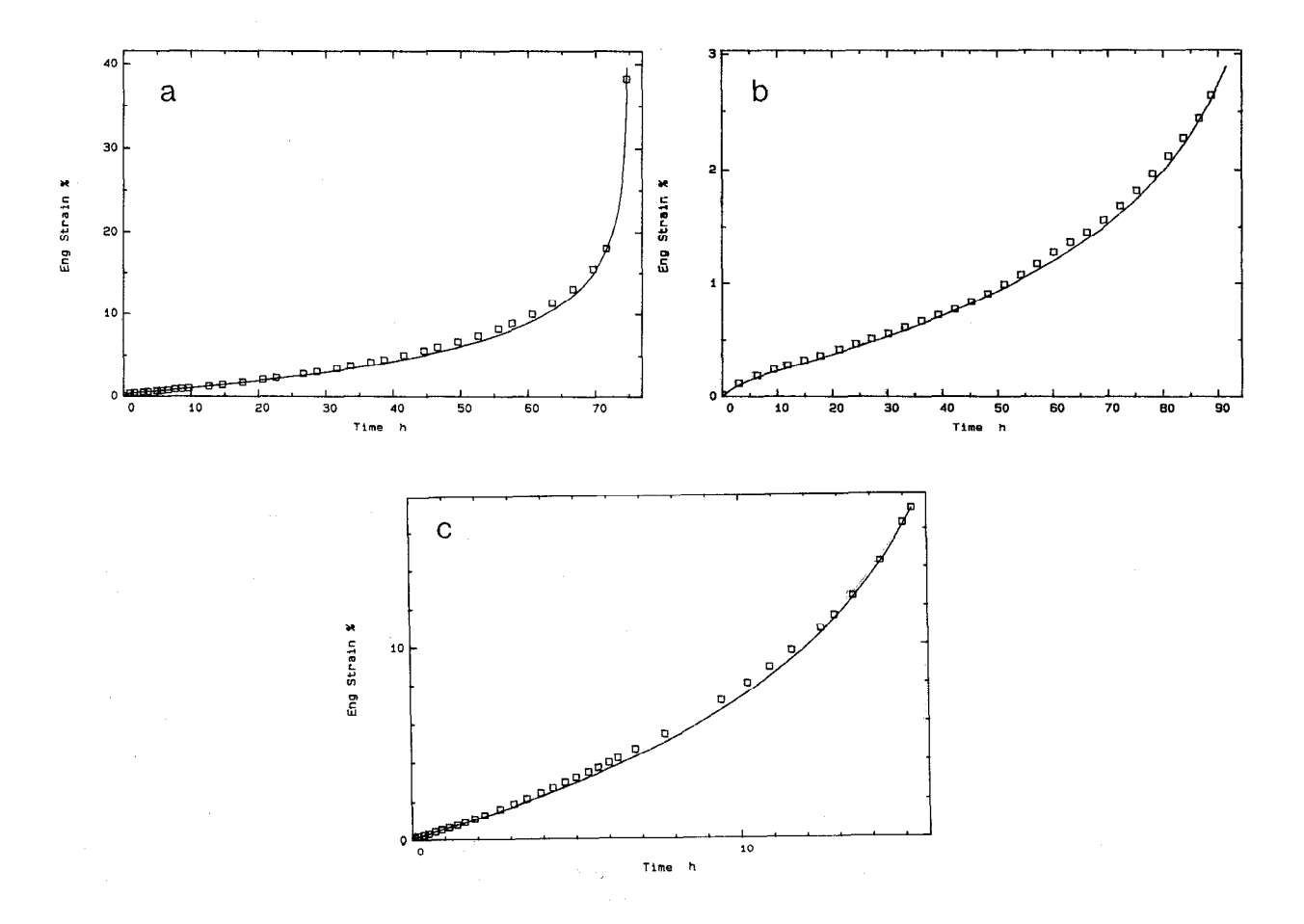


Figure 3 Examples of the agreement between experimental data (points) and the CRISPEN representation (line)

- a) IN738LC, directionally solidified, constant load 375 MPa/850 °C
- b) MarM002, conventionally cast, constant stress 240 MPa/950°C
- c) SRR99, single crystal, constant stress 600 MPa/900°C

Figure 3 shows the agreement between the creep curves calculated using Equations 10 together with the model parameters derived by these procedures and the original creep data. Examples are shown for (i) constant load creep tests for directionally solidified IN738LC where the contribution of loss of internal section is insignificant, (ii) constant stress tests on MarM002 where low ductility is due to extensive grain boundary cavitation and (iii) single crystal SRR99 in constant stress conditions where crystal orientation is an important factor. Equation set 10 is clearly capable of representing the creep behaviour in all of these cases.

The parameter sets derived in this manner constitute a database representing the full shapes of the creep curves from which further calculations can be made. Inspection of Figure 3 shows that primary creep is relatively unimportant for most long term tests. The tertiary behaviour and the life are largely controlled by the model parameters $\dot{\epsilon}_i \sim \dot{\epsilon}_{min}$ and C. The procedures adopted for representing $\dot{\epsilon}_{min}$ as a function of stress and temperature in terms of power or exponential laws are well known and will not be discussed further here. Figure 4a shows that for directionally solidified IN738LC C(\approx C_{int} + n) is relatively constant over a wide range of stresses and temperature. However, for MarM002 a variable C can be associated with differences in creep ductility, as shown in Figure 4b, indicating the dominance of loss of internal section by cavitation: from Equation 9, $C \sim n/3 \epsilon_f$.

Predictive Calculations

The procedure used by CRISPEN is to base predictions of creep curves for arbitrary stress/temperature conditions on the known model parameters for a reference creep curve at a neighbouring condition. It is assumed that the values of H, S_{SS} and C for the arbitrary condition are identical to those for the reference curve, but an appropriate value of $\dot{\epsilon}_1$ is calculated from the representation of $\dot{\epsilon}$ (σ ,T). In practice, the reference curve would be chosen to have a stress and temperature as close to the unknown condition as possible.

The following illustrations indicate extrapolations in time and to cyclic test conditions and compare the predictions with available experimental data.

- a) Figure 5 shows a series of calculated creep curves for directionally solidified IN738LC using the data for a test at 200 MPa/1223K, which had a life of ~ 50h, as a reference. The predictions are displayed as bands of ± 10% in life. Extrapolations across stress and/or temperature to times of up to ~ 20,000h give agreement within this range.
- b) The use of a single reference curve to predict the strain/time behaviour in conditions of changing stress and temperature are shown in Figures 6a and 6b respectively for directionally solidified IN738LC. Good agreement is obtained for these relatively small changes in test conditions. However, this should <u>not</u> be taken to indicate that CRISPEN is appropriate to calculate fatigue behaviour.
- c) It is difficult to evaluate the overall self-consistency of such predictions from isolated comparisons. Figure 7 shows a Larson-Miller plot constructed for conventionally cast MarM002 by using CRISPEN to calculate lives for arbitrarily chosen conditions of stress and temperature using the available database. Experimental points for the tests constituting the database are shown for reference. The scatter in this predicted Larson-Miller plot of ~ ± 10% in stress is no greater than the inherent scatter of the experimental data or of the normal scatter found in such parametric representations used for design purposes. The ability of CRISPEN to generate acceptable Larson-Miller curves provides confirmation of the reliability of the strain/time predictions.

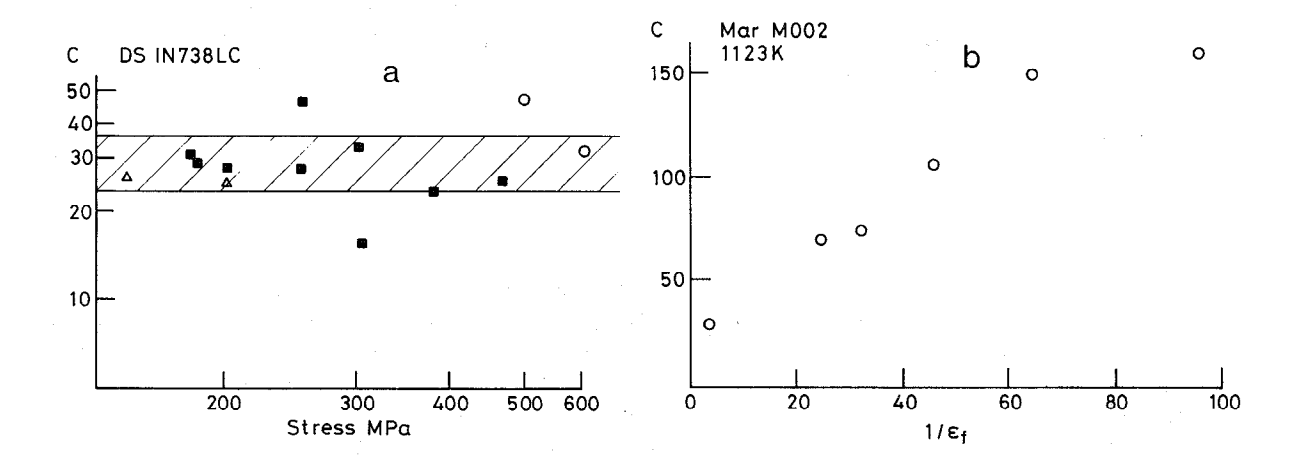


Figure 4 a) Tertiary creep parameter C for directionally solidified IN738LC as a function of stress and temperature. b) Tertiary creep parameter C for conventionally cast MarM002 shown as a function of $1/\epsilon_{\rm f}$.

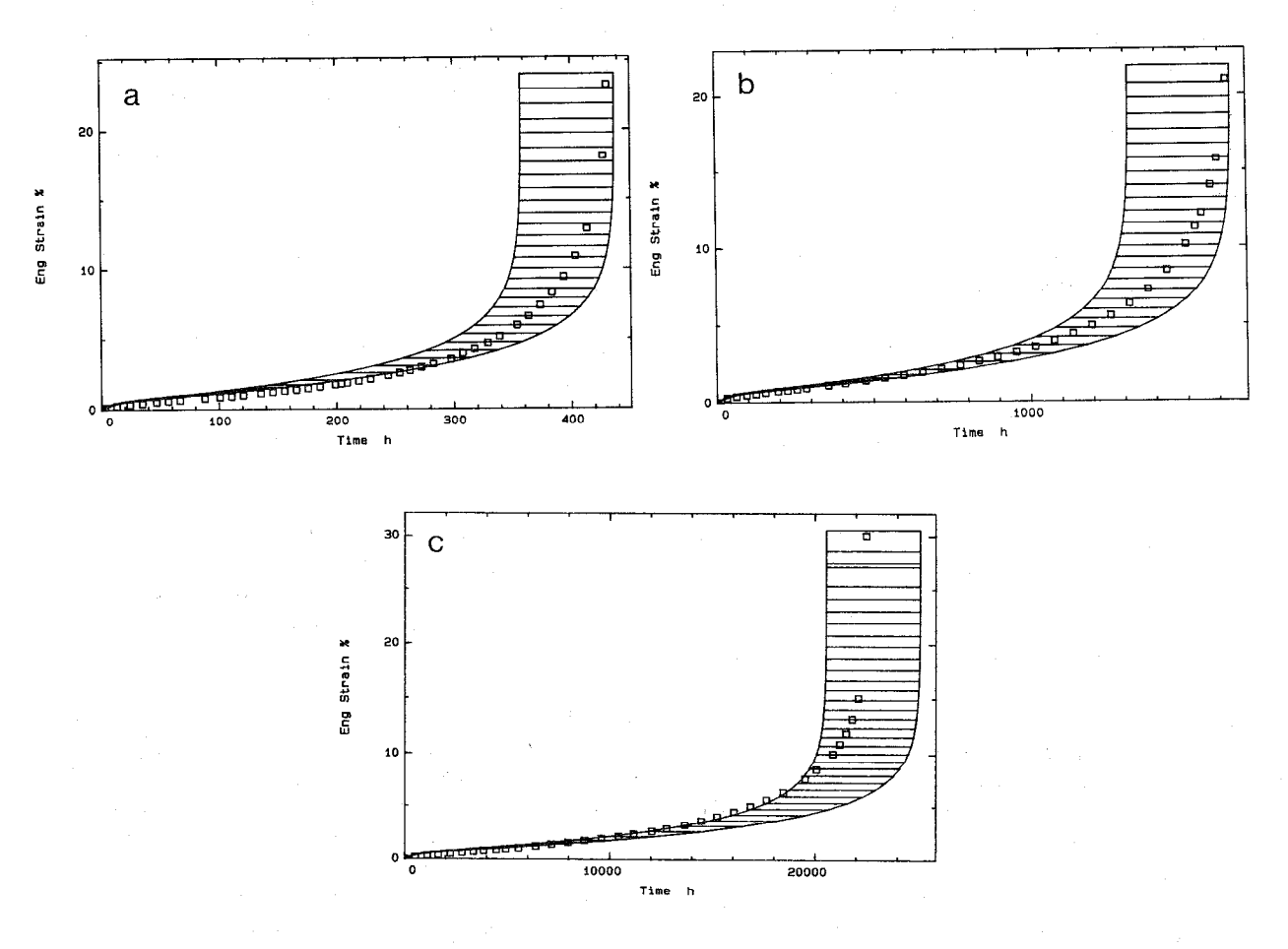


Figure 5 Comparison of experimental creep data with CRISPEN generated creep curves calculated using short term reference data (viz 200 MPa, 950 $^{\circ}$ C, t_f =40h).

- a) 150 MPa, 950°C
- b) 250 MPa, 850°C
- c) 170 MPa, 850°C.

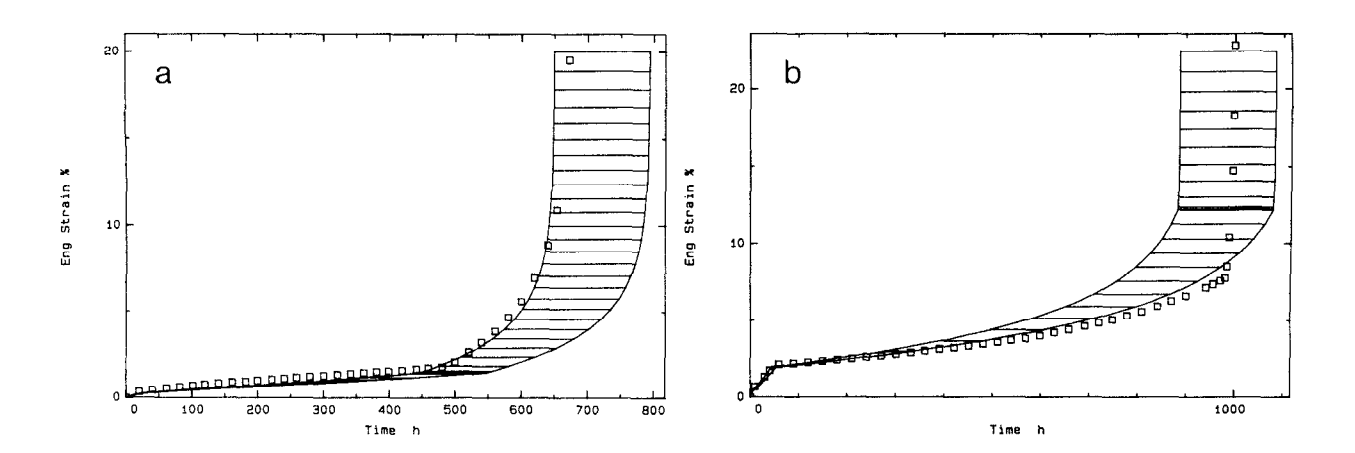


Figure 6 As Figure 5 but for conditions of changing stress and temperature a) $\sigma_1 = 250$ MPa, 0 - 497 h; $\sigma_2 = 300$ MPa, 497 - 672.5 h; T = 850°C b) $T_1 = 900$ °C, 0 - 49.5 h; $T_2 = 850$ °C, 495 - 9815 h; $T_3 = 900$ °C, 981.5 - 999.2 h; $\sigma = 250$ MPa.

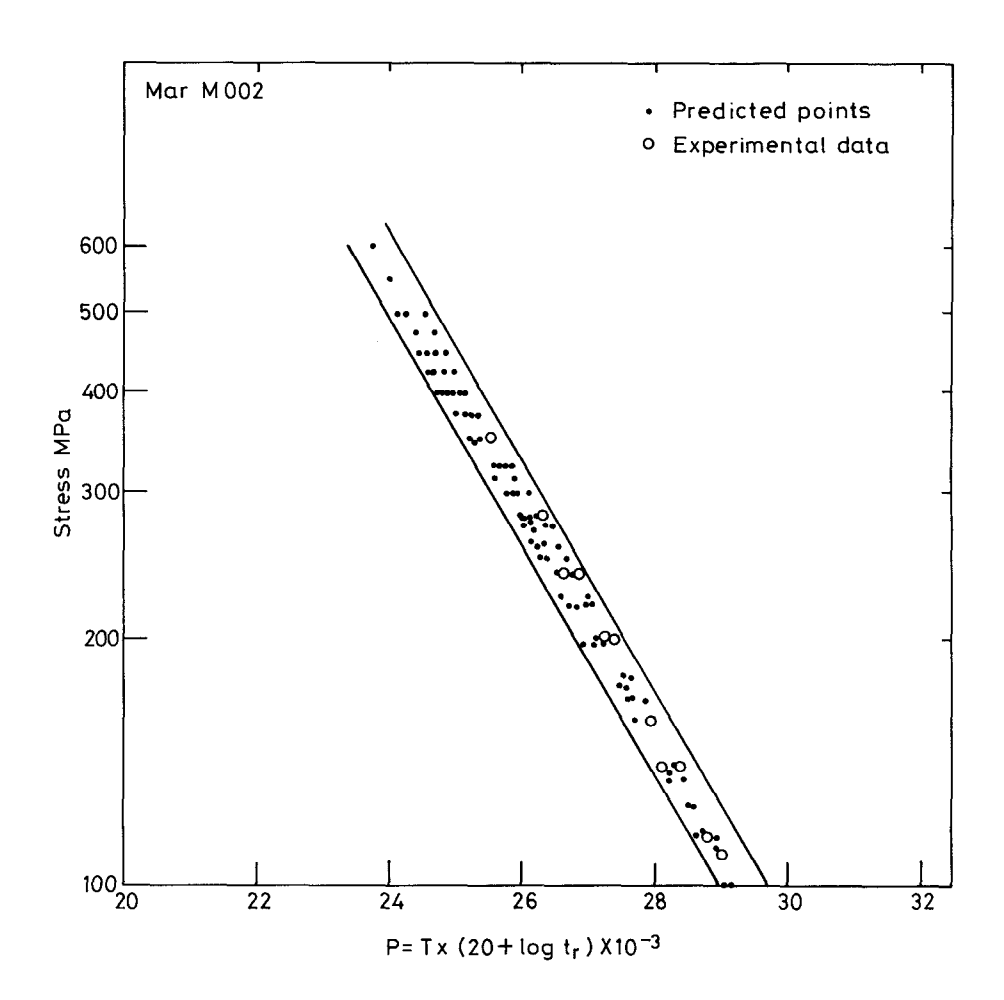


Figure 7 Larson-Miller plot for conventionally cast MarM002 calculated from the CRISPEN database for random stress/temperature conditions. Experimental data are included for comparison.

Conclusions

- 1. Constitutive laws, expressed in the formalism of continuum damage mechanics, with clear physical meaning are capable of representing the shapes of creep curves for superalloys in both constant and cyclic stress/temperature conditions.
- 2. A computer package (CRISPEN) has been developed to operate on these equations which is able to:
 - o analyse creep curves
 - o compile a database to represent the full shape of a creep curve
 - o simulate a creep curve for an arbitrary condition from the database
 - o compare a simulated curve with available data
- 3. The system has been evaluated on data for several nickel-base superalloys.

Acknowledgements

The authors thank Drs J C Ion and M Maldini for contributions at various stages of this NPL/Cambridge University collaborative programme.

References

- 1. L.M. Brown (1982) 3rd Risó Int. Symposium. "Fatigue and Creep of Composite Materials" (Eds H. Lilholt and R. Talrega) p.1.
- 2. B.F. Dyson and M. McLean (1983) Acta Metall., 31, 17.
- 3. B.F. Dyson and T.B. Gibbons (1987) Acta Matall., 35, 2355.
- 4. J.C. Ion, A. Barbosa, M.F. Ashby, B.F. Dyson and M. McLean. NPL Report DMA A115, April 1986.
- 5. G.A. Webster, A.P.D. Cox and J.E. Dorn (1969) Met. Sci. Jnl. 3, 221.
- 6. R.W. Evans, J.D. Parker and B. Wilshire (1982) in "Recent Advances in Creep and Fracture of Engineering Materials and Structures (Eds B. Wilshire and D.R.J. Owen) Pineridge Press Swansea, p.135.
- 7. M.F. Ashby and B.F. Dyson (1984) ICF6 New Delhi, Pergamon, p.3.
- 8. H. Burt, J.P. Dennison and B. Wilshire (1979) Metal Sci. 13, 295.
- 9. P.J. Henderson and M. McLean 1983 Acta Metall., 31, 1203.
- 10. P.N. Quested, P.J. Henderson and M. McLean. Acta Metall., (in press).
- 11. L.M. Kachanov (1958). Izv. Akad. Nank. SSSR No.8, 26.
- 12. F.A. Leckie and D.R. Hayhurst (1977) Acta Metall., 25, 1059.
- 13. Yu.N. Rabotnov (1969). Proc. XII IUTAM Congress, Stanford, Eds. Hetenyi and W.G. Vincenti, Springer, p.342.
- 14. J. Hult (1974) In "On Topics in Applied Continuum Mechanics" (Eds. J.L. Zeman and F. Ziegler) Springer p.137.
- 15. N.G. Taylor and M.F. Ashby work to be published.